

Reactivity of Chromium(III) Nutritional Supplements in Biological Media: An X-Ray Absorption Spectroscopic Study

Annie Nguyen, Irma Mulyani, Aviva Levina, and Peter A. Lay*

School of Chemistry, The University of Sydney, NSW, 2006, Australia

Received December 17, 2007

Chromium(III) nutritional supplements are widely used due to their purported ability to enhance glucose metabolism, despite growing evidence on low activity and the potential genotoxicity of these compounds. Reactivities of Cr(III) complexes used in nutritional formulations, including $[\text{Cr}_3\text{O}(\text{OCOEt})_6(\text{OH}_2)_3]^+$ (**A**), $[\text{Cr}(\text{pic})_3]$ (pic = 2-pyridinecarboxylato(−)) (**B**), and *trans*- $[\text{CrCl}_2(\text{OH}_2)_4]^+$ ($\text{CrCl}_3 \cdot 6\text{H}_2\text{O}$; **C**), in a range of natural and simulated biological media (artificial digestion systems, blood and its components, cell culture media, and intact L6 rat skeletal muscle cells) were studied by X-ray absorption near-edge structure (XANES) spectroscopy. The XANES spectroscopic data were processed by multiple linear-regression analyses with the use of a library of model Cr(III) compounds, and the results were corroborated by the results of X-ray absorption fine structure spectroscopy and electrospray mass spectrometry. Complexes **A** and **B** underwent extensive ligand-exchange reactions under conditions of combined gastric and intestinal digestion (in the presence of a semisynthetic meal, 3 h at 310 K), as well as in blood serum and in a cell culture medium (1–24 h at 310 K), with the formation of Cr(III) complexes with hydroxo and amino acid/protein ligands. Reactions of compounds **A–C** with cultured muscle cells led to similar ligand-exchange products, with at least part of Cr(III) bound to the surface of the cells. The reactions of **B** with serum greatly enhanced its propensity to be converted to Cr(VI) by biological oxidants (H_2O_2 or glucose oxidase system), which is proposed to be a major cause of both the insulin-enhancing activity and toxicity of Cr(III) compounds (Mulyani, I.; Levina, A.; Lay, P. A. *Angew. Chem. Int. Ed.* **2004**, *43*, 4504–4507). This finding enhances the current concern over the safety of consumption of large doses of Cr(III) supplements, particularly $[\text{Cr}(\text{pic})_3]$.

Introduction

Chromium(III) nutritional supplements, primarily $[\text{Cr}(\text{pic})_3]$ (pic = picolinato(−) = 2-pyridinecarboxylato(−)), have been actively promoted since the 1980s as a means of enhancing glucose metabolism, fat reduction, and muscle building and have since reached second place in the supplement market (after Ca(II) salts).¹ However, the benefits of Cr(III) supplementation for healthy people, as well as the essentiality of Cr(III) for glucose metabolism in humans, have been seriously questioned in recent years.¹ No well-defined Cr(III)-dependent enzymes or cofactors are known as yet, and the mechanisms of Cr(III) action as an insulin-enhancing agent remain unclear.^{2,3} Beneficial effects of Cr(III) compounds

on glucose metabolism seem to be limited to type II diabetes patients taking very large doses of the supplements (≥ 1 mg of Cr per day), which exceed by 30–40-fold the currently accepted values of adequate dietary intakes of Cr.⁴ Since $[\text{Cr}(\text{pic})_3]$ is known to be genotoxic and mutagenic at high concentrations,^{4,5} a number of alternative Cr(III) supplements have been proposed. These include trinuclear Cr(III) propionate ($[\text{Cr}_3\text{O}(\text{OCOEt})_6(\text{OH}_2)_3]^+$), which has been shown to reduce cholesterol and triglyceride levels in the blood of healthy and type II diabetic rats,⁶ and has been proposed as a structural and functional mimetic of a purported natural Cr(III)-containing peptide, chromodulin.^{2,7} Inorganic Cr(III)

* Author to whom correspondence should be addressed. Tel.: 61-2-9351 4269. Fax: 61-2-9351 3329. E-mail: p.lay@chem.usyd.edu.au.

(1) Vincent, J. B. In *The Nutritional Biochemistry of Chromium(III)*; Vincent, J. B., Ed.; Elsevier: Amsterdam, 2007; pp vii–ix.
(2) Vincent, J. B. In *The Nutritional Biochemistry of Chromium(III)*; Vincent, J. B., Ed.; Elsevier: Amsterdam, 2007; pp 139–162.

(3) Stearns, D. M. In *The Nutritional Biochemistry of Chromium(III)*; Vincent, J. B., Ed.; Elsevier: Amsterdam, 2007; pp 57–70.

(4) Stearns, D. M. In *The Nutritional Biochemistry of Chromium(III)*; Vincent, J. B., Ed.; Elsevier: Amsterdam, 2007; pp 209–225.

(5) (a) Coryell, V. H.; Stearns, D. M. *Mutat. Res.* **2006**, *610*, 114–123.
(b) Andersson, M. A.; Petersson Grawé, K. V.; Karlsson, O. M.; Abramson-Zetterberg, L. A. G.; Hellman, B. E. *Food Chem. Toxicol.* **2007**, *45*, 1097–1106.

salts (usually $\text{CrCl}_3 \cdot 6\text{H}_2\text{O}$) are used in some nutritional formulations⁸ and in many *in vitro* studies on the biological effects of Cr(III).⁹

The widespread use of Cr(III) complexes in nutrition raises the problem of their stability and speciation in biological media, such as stomach and intestinal fluids, blood plasma, or intact cells. Typical metabolic pathways of metal complexes, including ligand-exchange and redox reactions, are more complicated than those of organic drugs and are often ignored in studies of the biological activities of metal ions.¹⁰ X-ray absorption spectroscopy (XAS), including X-ray absorption near-edge structure (XANES) and X-ray absorption fine structure (XAFS) spectroscopies, provides a selective and sensitive tool for the studies of changes in coordination environments of metal ions in biological samples.¹¹ For instance, multiple linear-regression analyses of XANES spectra, using a library of model Cr(III) compounds, enabled the average coordination environments of Cr(III) complexes formed in Cr(VI)-treated mammalian cells to be proposed.¹² In the current work, the same method (in combination with XAFS spectroscopy and analytical techniques) was applied to studies of chemical transformations of Cr(III) nutritional supplements in natural and simulated biological media, including artificial digestion systems, blood and its components, a cell culture medium, and intact mammalian cells. An insulin-sensitive rat skeletal muscle cell line (L6)¹³ was chosen in connection with the proposed roles of Cr(III) in insulin signaling and glucose metabolism,² since skeletal muscle tissue is responsible for up to 75% of insulin-dependent glucose transport in mammals.¹⁴ Reactivity of Cr(III) biotransformation products toward biological oxidants (H_2O_2 or glucose oxidase system) in blood serum was studied in relation to the recent hypothesis^{10,15} that

Table 1. Designations of the Initial or Model Cr(III) Complexes

designation	description ^a	ref
A	$[\text{Cr}_3\text{O}(\text{OCOEt})_6(\text{OH}_2)_3](\text{NO}_3) \cdot 3\text{H}_2\text{O}$	17
B	$[\text{Cr}(\text{pic})_3] \cdot \text{H}_2\text{O}$	18
C	<i>trans</i> - $[\text{CrCl}_2(\text{OH}_2)_4]\text{Cl} \cdot 2\text{H}_2\text{O}^b$	22
D	$\text{Na}[\text{Cr}(\text{asp})_2] \cdot 2\text{H}_2\text{O}^c$	19
E	$[\text{Cr}(\text{his})_2](\text{BF}_4)^c$	20
F	$\text{Na}_9[\text{Cr}(\text{OH})_6]_2(\text{OH})_3 \cdot 6\text{H}_2\text{O}$	21
G	$\text{Cr}(\text{III})-\text{OH}-\text{OH}_2$ dimer/trimer	23

^a Designations of the ligands: pic = 2-pyridinecarboxylato(-); asp = L-aspartato(2-); his = L-histidinato(-). ^b Commercial $\text{CrCl}_3 \cdot 6\text{H}_2\text{O}$ (Merck). ^c Data for mixtures of geometric isomers were used in the analyses; no significant differences in XANES spectra of separate geometric isomers were detected.¹²

biological oxidation of Cr(III) to Cr(VI/V) species is responsible for its insulin-enhancing activities.

Experimental Section

Caution! Chromium(VI) compounds are human carcinogens;¹⁶ skin contacts and inhalation must be avoided.

Materials. Analytical or higher-grade reagents were purchased from Merck or Sigma-Aldrich and were used without further purifications. Water was purified by the MilliQ technique. Pre-sterilized solutions and sterile disposable plasticware, used in cell culture work, were purchased from Gibco and Becton Dickinson, respectively. A list of Cr(III) compounds (**A–G**), used in sample preparation, or as models in final XANES data analyses, is given in Table 1. Syntheses (by modified literature procedures)^{17–21} and characterization of the complexes **A**, **B**, **D**, **E**, and **F** were described previously.¹² Complex **C** ($\text{CrCl}_3 \cdot 6\text{H}_2\text{O}$, >99%)²² was purchased from Merck. A mixture of Cr(III) aqua-hydroxo oligomers²³ was generated by the reaction of aqueous $[\text{Cr}(\text{OH}_2)_6]^{3+}$ ($\text{Cr}(\text{NO}_3)_3 \cdot 9\text{H}_2\text{O}$ from Merck, >99%; 0.10 M)²⁴ with NaOH (0.10 M) for 48 h at 295 K. An aliquot of the resultant solution (0.50 mL) was diluted 5-fold with H_2O , loaded to a column (1 cm \times 20 cm) of Sephadex G-25 (a size-exclusion resin, Amersham), and the complexes were eluted with water. The main chromatographic fraction, containing mostly dimeric and trimeric Cr(III) species (as determined by electronic absorption spectroscopy, see Results),²³ was freeze-dried (217 K and 0.5 mbar for 15 h) and used for XANES spectroscopy (**G** in Table 1). The stability of the resultant Cr(III) complexes during freeze-drying was confirmed by electronic absorption spectroscopy (see Results).

Sample Preparation. Table 2 presents a summary of reaction conditions used in the reactivity studies of Cr(III) complexes **A–C** (Table 1) in biological media (conditions 1–7 in Table 2 were used for **A** and **B** only, and condition 8 was used for **A** only). In a typical experiment (conditions 1–9 in Table 2), a Cr(III) compound ($[\text{Cr}] = 1.0$ or 0.10 mM) was reacted with a natural or simulated biological fluid for a specified time (Table 2) at 310 K; then, the reaction mixture was frozen in liquid N_2 and freeze-dried (217 K

- (6) (a) Sun, Y. J.; Clodfelder, B. J.; Shute, A. A.; Irvin, T.; Vincent, J. B. *J. Biol. Inorg. Chem.* **2002**, *7*, 852–862. (b) Clodfelder, B. J.; Gullick, B. M.; Lukaski, H. C.; Neggers, Y.; Vincent, J. B. *J. Biol. Inorg. Chem.* **2005**, *10*, 119–130.
- (7) Davis, C. M.; Royer, A. C.; Vincent, J. B. *Inorg. Chem.* **1997**, *36*, 5316–5320.
- (8) (a) Inceli, M. S.; Bolckert, S.; Doger, M. M.; Yanardag, R. *Mol. Cell. Biochem.* **2007**, *294*, 37–44. (b) Mao, F. C.; Chen, W.-Y.; Cheng Chiang, L.-H. *Chem. Abstr.* **2007**, *146*, 115035; Composition for Preventing and Treating Cardiovascular Disorders, U.S. Patent 2007010426, 2007.
- (9) (a) Morris, B.; Gray, T.; MacNeil, S. *J. Endocrinol.* **1995**, *144*, 135–141. (b) Goldstein, B. J.; Zhu, L.; Hager, R.; Zilbering, A.; Sun, Y.; Vincent, J. B. *J. Trace Elem. Exp. Med.* **2001**, *14*, 393–404. (c) Jain, S. K.; Lim, G. *Horm. Metab. Res.* **2006**, *38*, 60–62.
- (10) (a) Levina, A.; Mulyani, I.; Lay, P. A. In *The Nutritional Biochemistry of Chromium(III)*; Vincent, J. B., Ed.; Elsevier: Amsterdam, 2007; pp 225–257. (b) Levina, A.; Lay, P. A. *Chem. Res. Toxicol.* **2008**, *21*, 563–571.
- (11) (a) Levina, A.; Armstrong, R. S.; Lay, P. A. *Coord. Chem. Rev.* **2005**, *249*, 141–160. (b) Gunter, K. K.; Miller, L. M.; Aschner, M.; Eliseev, R.; Depuis, D.; Gavin, C. E.; Gunter, T. E. *Neurotoxicology* **2002**, *23*, 127–146. (c) Levina, A.; McLeod, A. I.; Seuring, J.; Lay, P. A. *J. Inorg. Biochem.* **2007**, *101*, 1586–1593.
- (12) Levina, A.; Harris, H. H.; Lay, P. A. *J. Am. Chem. Soc.* **2007**, *129*, 1065–1075; **2007**, *129*, 9832.
- (13) (a) Sarabia, V.; Ramlal, T.; Klip, A. *Biochem. Cell Biol.* **1990**, *68*, 536–542. (b) Elsner, P.; Quistoff, B.; Hermann, T. S.; Dich, J.; Grunett, N. *Am. J. Physiol.* **1998**, *275*, E925–E933. (c) L6 rat skeletal muscle cell line (ATCC No. CRL-1458).
- (14) Saltiel, A. R.; Kahn, C. R. *Nature* **2001**, *114*, 799–806.
- (15) Mulyani, I.; Levina, A.; Lay, P. A. *Angew. Chem., Int. Ed.* **2004**, *43*, 4504–4507.

- (16) *Overall Evaluations of Carcinogenicity to Humans*; International Agency for Research on Cancer: Lyon, France, 2003.
- (17) Antsyshkina, A. S.; Porai-Koshits, M. A.; Arkhangel'skii, I. V.; Diallo, I. N. *Russ. J. Inorg. Chem.* **1987**, *32*, 2928–2932; English Translation pp 1700–1703.
- (18) Stearns, D. M.; Armstrong, W. H. *Inorg. Chem.* **1992**, *31*, 5178–5184.
- (19) Watabe, M.; Yano, H.; Odaka, Y.; Kobayashi, H. *Inorg. Chem.* **1981**, *20*, 3623–3627.
- (20) Hoggard, P. E. *Inorg. Chem.* **1981**, *20*, 415–420.
- (21) Hinz, D. Z. *Anorg. Allg. Chem.* **2000**, *626*, 1004–1011.
- (22) Bussièrè, G.; Beaulac, R.; Cardinal-David, B.; Reber, C. *Coord. Chem. Rev.* **2001**, *219*, 509–543.
- (23) Stünzi, H.; Marty, W. *Inorg. Chem.* **1983**, *22*, 2145–2150.
- (24) Lazar, D.; Ribar, B.; Divjakovic, V.; Meszaros, C. *Acta Crystallogr., Sect. C* **1991**, *C47*, 1060–1062.

Table 2. Conditions Used for Sample Preparation^a

no.	description
1	simulated gastric juice (pH ~ 2, 24 h)
2	simulated intestinal fluid (pH ~ 8, 24 h)
3	artificial gastric digestion with semisynthetic meal (1 h)
4	artificial gastric and intestinal digestion with semisynthetic meal (3 h)
5	rat serum (1 h)
6	rat serum (6 h)
7	rat serum (24 h)
8	intact rat blood (24 h), then plasma separated
9	cell culture medium with 2% fetal calf serum (20 h, [Cr] = 0.10 mM)
10	L6 rat myotubes were treated with Cr(III) (0.10 mM, 20 h)
11	Cr(III) (0.10 mM) was reacted with RSA (24 h), then unbound Cr(III) was removed ^b

^a All of the treatments were carried out at 310 K. Unless stated otherwise, concentrations of Cr(III) in solutions before freeze-drying were 1.0 mM. Details of the treatments are given in the Experimental Section. ^b RSA = rat serum albumin. Similar reactions were also performed with bovine apo-transferrin (see the Supporting Information). The reactions were carried out in HBS (containing 20 mM HEPES, pH 7.4, and 0.14 M NaCl). Unbound Cr(III) was removed on Microcon YM-30 membrane filters (see the Experimental Section).

and 0.5 mbar for 15 h), and the resultant solid was stored desiccated at 277 K for 1–2 weeks prior to analyses. Stock solutions of **A** or **C** in H₂O ([Cr] = 0.10 M) were prepared immediately before the experiments. Due to the poor solubility of **B**, its solutions in aqueous buffers or in blood serum were prepared by sonication (10 min at 50 W and 298 K), and undissolved solid was removed by centrifugation (~1 min at 10 000g and 298 K). The concentration of **B** in saturated solutions ([Cr] = 1.0 ± 0.1 mM) was determined by atomic absorption spectroscopy (AAS).

Simulated gastric juice (pH ~ 2, condition set 1 in Table 2) contained NaCl (0.15 M) and HCl (0.05 M).²⁵ Simulated intestinal fluid (pH ~ 8, condition set 2 in Table 2) contained NaCl (0.15 M) and NaHCO₃ (10 mM).²⁵ Modified literature methods²⁶ were used for the preparation of a semisynthetic meal and for artificial digestion experiments (conditions 3 and 4 in Table 2). Bovine serum albumin (3.68 g), soluble starch (6.68 g), sunflower seed oil (3.48 g), calcium lactate (0.076 g), and K₂HPO₄ (0.29 g) were mixed with H₂O (20 mL) in a food blender, to produce a stable emulsion (~30 mL, pH = 6.8). The pH value was adjusted to 2.0 with HCl (10 M), and porcine pepsin (2.0 mg per mL of emulsion, dissolved in a minimal amount of 0.10 M HCl) was added. Aliquots (1.0 mL) of the resultant emulsion, used to simulate a stomach environment, were mixed with compounds **A** or **B** (final [Cr] = 1.0 mM), and the mixtures were incubated for 1 h at 310 K in a rocking water bath. The resultant reaction mixtures were divided into two groups. In the first group (artificial gastric digestion, condition set 3 in Table 2), insoluble parts of the reaction mixtures were separated by centrifugation (1000g for 5 min at 295 K), and the supernatants were freeze-dried for XANES spectroscopy. The remaining samples (combined gastric and intestinal digestions, condition set 4 in Table 2) were brought to pH ~ 6.0 by additions of aqueous NaHCO₃ (1.0 M). Porcine pancreatin solution (0.50 mg per mL of emulsion, dissolved in a minimal amount of 0.10 M NaHCO₃) was then added to the mixtures, followed by the addition of aqueous NaOH (1.0 M) to the final pH value of ~7.0. The resultant mixtures were used to simulate an intestinal environment

and were incubated for 2 h at 310 K in a rocking water bath, then processed as described above.

Blood samples were collected on the day of experiments from healthy male Sprague–Dawley rats. Animal handling was in accordance with University of Sydney animal ethics approval (L07/1-2004/3/3846). Whole blood samples were collected into heparin-coated Vacutainer tubes (Becton Dickinson). Blood samples for serum separation were collected into Corvac tubes (Tyco Healthcare), equipped with wax plugs, and immediately centrifuged at 1000g (10 min at 295 K). The resultant serum was decanted from the tubes, heat-treated (30 min at 329 K) to minimize enzyme activity,²⁷ and stored at 277 K for no longer than 3 days. In the reaction of **A** with whole blood (condition set 8 in Table 2), red blood cells (RBCs) and plasma were isolated (by centrifugation for 10 min at 1000g and 295 K) after the Cr(III) treatment, and then freeze-dried separately. This experiment was not performed for **B**, since this compound could only be dissolved in aqueous media by sonication, and this led to extensive damage of the RBCs.

A culture of L6 rat muscle cells (myoblasts)¹³ was obtained from Dr. Amira Klip, The Hospital for Sick Children, Toronto, Canada. The cells were cultured in monolayers in a minimal essential medium containing L-glutamine, ribonucleosides, and deoxyribonucleosides (α -MEM),²⁸ supplemented with an antibiotic–antimycotic mixture (100 U mL⁻¹ penicillin, 100 mg mL⁻¹ streptomycin, and 0.25 mg mL⁻¹ amphotericin B) and fetal calf serum (FCS; heat-inactivated, 10% v/v). The cells at passage 7–11 were seeded at a density of 2 × 10⁵ cells per 100-mm tissue culture dish in 10 mL of medium, grown to ~60% confluency at 310 K in a humidified incubator (5% CO₂), and subcultured every 2–3 days. Differentiation of L6 cells was induced by growing the cells to 100% confluency in α -MEM with 10% v/v FCS, then reducing the amount of FCS to 2% v/v, and changing the medium every 2 days for 9–10 days.¹³ During this time, >95% of the myoblasts were fused into myotubes (mature skeletal muscle cells).¹³ Differentiated cells were treated with Cr(III) compounds **A–C** (0.10 mM for 20 h at 310 K, condition set 10 in Table 2) or with Cr(VI) (10 μ M Na₂CrO₄ for 20 h at 310 K) in a complete medium with FCS (2% v/v). None of the treatments caused visible changes in cell morphology. Cell pellets were collected after the treatments and prepared for XANES spectroscopy, as described previously.^{12,29} Aliquots (1.0 mL) of the cell culture medium after the Cr(III) treatments were also collected and freeze-dried for XANES spectroscopy (condition set 9 in Table 2).

Adducts of compounds **A–C** with rat serum albumin (RSA; condition set 11 in Table 2) or bovine apo-transferrin were prepared by the reactions of the proteins (5.0 mg mL⁻¹) with the Cr(III) compounds ([Cr] = 0.10 mM) in HEPES-buffered saline (HBS; where HEPES is 4-(2-hydroxyethyl)-1-piperazine-ethanesulfonic acid), containing HEPES (20 mM, pH = 7.4) and NaCl (0.14 M) for 24 h at 310 K. In order to remove the unbound Cr(III), the reaction mixtures were then passed through Microcon YM 30 membrane filters (Millipore; 30 kDa cutoff; volume, 0.50 mL) by centrifugation (14 000g for 30 min at 295 K). The residues on the filters were washed twice with HBS (0.50 mL), collected, and freeze-dried for XANES spectroscopy.

X-Ray Absorption Spectroscopy (XAS) and Data Analysis. Chromium K-edge spectra were recorded at beamline 9-3 at the Stanford Synchrotron Radiation Laboratory (SSRL) or at the Australian National Beamline Facility (ANBF; beamline 20B at

(25) Gammelgaard, B.; Joens, O. In *Handbook of Metal-Ligand Interactions in Biological Fluids: Bioinorganic Medicine*; Berthon, G., Ed.; Marcel Dekker: New York, 1995; Vol. 1, pp 48–61.

(26) (a) Glahn, R. P.; Lee, O. A.; Yeung, A.; Goldman, M. I.; Miller, D. D. *J. Nutr.* **1998**, *128*, 1555–1561. (b) Yun, S.; Habicht, J.-P.; Miller, D. D.; Glahn, R. P. *J. Nutr.* **2004**, *134*, 2717–2721.

(27) Animal Sera (general description); Gibco, Invitrogen Corp.

(28) α -MEM, Cat. No. 12571-071; Gibco, Invitrogen Corp.

(29) Harris, H. H.; Levina, A.; Dillon, C. T.; Mulyani, I.; Lai, B.; Cai, Z.; Lay, P. A. *J. Biol. Inorg. Chem.* **2005**, *10*, 105–118.

the Photon Factory, Tsukuba, Japan). The beam energy was 3.0 GeV (SSRL) or 2.5 GeV (ANBF), and the maximal beam current was 100 mA (SSRL) or 400 mA (ANBF). Beamline 9-3 at SSRL had a double-crystal Si[220] monochromator, an upstream collimating mirror, and a downstream sagittally focusing mirror; both mirrors were Rh-coated and also provided harmonic rejection. Harmonic rejection was achieved at ANBF by detuning the channel-cut Si[111] monochromator by 50%. Neat freeze-dried biological samples (Table 2) or mixtures of model complexes with BN (~1:10 w/w) were pressed into 0.5-mm pellets that were supported within an Al spacer between two 63.5- μm Kapton tape windows (window size, 2×10 mm), and XAS data were recorded at 295 K. Low-temperature XAS measurements could not be used for most of the biological samples due to the low Cr concentrations and strong absorption of photons at the ~ 6 keV energy range by cryostat windows.²⁹ All XAS data were acquired in fluorescence detection mode, using a 30-element Ge-array detector (Canberra Industries) at SSRL or a 36-pixel Ge planar detector (Eurisys) at ANBF. For most samples, XANES spectra were recorded at SSRL or ANBF at the 5770–6200 eV energy range (step sizes, 10 eV below 5970 eV, 0.25 eV above 5970, and 5 eV above 6100 eV). The energy scale was calibrated using a stainless steel foil as an internal standard (calibration energy, 5989.0 eV, corresponded to the first peak of the first derivative of Cr(0) edge).³⁰ Two sequential scans were recorded for each sample (scan time, 20 min), and the absence of noticeable photodamage of the samples was confirmed from the lack of significant spectral changes between the scans (e.g., the difference in edge energies did not exceed 0.1 eV).³¹ For some of the samples, both XANES and XAFS spectra were recorded at ANBF, using the following energy ranges: pre-edge region, 5770–5970 eV (10 eV steps); XANES region, 5970–6050 eV (0.25 eV steps); and XAFS region, 6050–7000 eV (0.05 \AA^{-1} steps in k space). For these samples, four to five sequential scans were recorded (scan time, 40 min), and the lack of appreciable photodamage was established from the absence of significant changes in XANES spectra of sequential scans.³¹ The possibility of sample photodamage is generally lower at ANBF compared with SSRL due to a lower photon flux.³¹

Calibration, averaging, and splining of XANES data were performed using the XFit software package.³² For the analysis of XANES features, the spectra were normalized (using the Spline program within the XFit package) according to the method of Penner-Hahn and co-workers,³³ to match the tabulated X-ray cross-section data³⁴ for Cr (illustrated in Figure S1, Supporting Information). This normalization technique led to consistent XANES spectra for all of the samples, regardless of the beamline used and the signal-to-noise ratio (see Figure S1, in the Supporting Information, and the Results section). Differentiation of XANES spectra and smoothing of the resultant first-derivative spectra were performed

using the Origin software.³⁵ A fast Fourier transform (FFT) smoothing procedure³⁵ was used; each point in the smoothed spectrum was calculated from 20 adjacent points in the first-derivative spectrum.^{11c} Multiple linear regression analyses of XANES data were also performed using the Origin software³⁵ with previously described criteria for a successful fit.¹² Single-scattering (SS) fittings of XAFS data were performed using the XFit software package,³² based on the FEFF8 code.³⁶ Overdetermined models ($N_i/p > 1$, where N_i is the number of independent observations and p is the number of varied parameters) were used in XAFS calculations, which allowed meaningful solutions to be obtained.³⁷ Published XANES data for the purported biologically relevant form of Cr “chromodulin”³⁸ were digitized using the WinDig software³⁹ for comparison with the data obtained in this work.

Analytical Techniques. Kinetics of Cr(III) (**A** or **B** in Table 1) oxidation to Cr(VI) by H_2O_2 or by the glucose oxidase/glucose/ O_2 system¹⁵ in rat serum or in aqueous buffer (HBS) were followed by measuring Cr(VI) concentrations spectrophotometrically with diphenylcarbazide (DPC; $\epsilon = 4.2 \times 10^4 \text{ M}^{-1} \text{ cm}^{-1}$ at 540 nm).⁴⁰ Typically, an aliquot of the reaction mixture (0.10 mL) was added to a solution (0.90 mL) of DPC (0.40 mM) in aqueous HCl (0.10 M); the absorbance at 540 nm was measured after 2 min (295 K); then, two to three aliquots (10 μL) of a standard Cr(VI) solution (1.00 mM) were added for calibration. The reaction of Cr(VI) with DPC was not affected by the presence of H_2O_2 (up to 5.0 mM in the undiluted reaction mixture). The formation of Cr(VI) in the reactions of Cr(III) complexes with oxidants was confirmed by the appearance of a characteristic $[\text{CrO}_4]^{2-}$ absorbance peak ($\lambda_{\text{max}} = 372 \text{ nm}$).¹⁵ Relative reactivities of **A** and **B** under various experimental conditions were reproduced in two independent experimental series; differences in the results of parallel experiments did not exceed 10–15%. Kinetic and electronic absorption spectroscopic measurements were performed on a Hewlett-Packard HP 8452A diode-array spectrophotometer (spectral range, 200–800 nm; resolution, 2.0 nm; acquisition time, 0.20 s).

Electrospray mass spectrometric (ESMS) studies of the decomposition of **A** in aqueous solutions at different pH values were performed using a Finnigan LCQ mass spectrometer. Typical experimental settings were as follows: sheath gas (N_2) pressure, 60 psi; spray voltage, 4.0 kV; capillary temperature, 473 K; cone voltage, 25 V; tube lens offset, 20 V; m/z range, 100–2000 (both in the positive- and negative-ion modes; no significant signals were detected in the latter mode). Analyzed solutions (5 μL , 1.0 mM Cr in 10 mM NH_3/AcOH buffers, pH = 4–9) were injected into a flow of $\text{H}_2\text{O}/\text{MeOH}$ (1:1 v/v, flow rate 0.20 mL min^{-1}). Acquired spectra were the averages of 10 scans (scan time 10 ms). Simulations of the mass spectra were performed using the IsoPro software.⁴¹

Chromium concentrations in the samples were determined either by graphite furnace atomic absorption spectroscopy (GFAAS; for Cr(III)-treated cell pellets), using a Varian SpecAA-20 spectrometer, or by an air– C_2H_2 flame AAS (for Cr(III) solutions in blood serum

(30) Thompson, A. C.; Attwood, D. T.; Gullikson, E. M.; Howells, M. R.; Kortright, J. B.; Robinson, A. L.; Underwood, J. H.; Kim, K.-J.; Kirz, J.; Lindau, I.; Pianetta, P.; Winick, H.; Williams, G. P.; Scofield, J. H. *X-Ray Data Booklet*, 2nd ed.; University of California: Berkeley, CA, 2001.

(31) (a) Rich, A. M.; Armstrong, R. S.; Ellis, P. J.; Freeman, H. C.; Lay, P. A. *Inorg. Chem.* **1998**, *37*, 5743–5753. (b) Levina, A.; Codd, R.; Foran, G. J.; Hambley, T. W.; Maschmeyer, T.; Masters, A. F.; Lay, P. A. *Inorg. Chem.* **2004**, *43*, 1046–1055.

(32) *XFit for Windows*, beta version; Australian Synchrotron Research Program: Sydney, Australia, 2004. <http://anbf2.kek.jp/xfit.html> (accessed Apr. 2008).

(33) Weng, T.-C.; Waldo, G. S.; Penner-Hahn, J. E. *J. Synchrotron Radiat.* **2005**, *12*, 506–510.

(34) McMaster, W. H.; Kerr Del Grande, N.; Mallett, J. H.; Hubbell, J. H. *Compilation of X-ray Cross Sections*; Lawrence Livermore National Laboratory: Livermore, CA, 1969; p 48.

(35) *Microcal Origin*, version 6.0; Microcal Software Inc.: Northampton, MA, 1999.

(36) Ankudinov, A. L.; Ravel, B.; Rehr, J. J.; Conradson, S. D. *Phys. Rev. B: Condens. Matter Mater. Phys.* **1998**, *58*, 7565–7576.

(37) Binsted, N.; Strange, R. W.; Hasnain, S. S. *Biochemistry* **1992**, *31*, 12117–12125.

(38) Jacquamet, L.; Sun, Y. J.; Hatfield, J.; Gu, W. W.; Cramer, S. P.; Crowder, M. W.; Lorigan, G. A.; Vincent, J. B.; Latour, J. M. *J. Am. Chem. Soc.* **2003**, *125*, 774–780.

(39) Lovy, D. *WinDIG*; University of Geneva: Geneva, Switzerland, 1996.

(40) Levina, A.; Bailey, A. M.; Champion, G.; Lay, P. A. *J. Am. Chem. Soc.* **2000**, *122*, 6208–6216.

(41) Senko, M. *IsoPro 3.0*; MS/MS Software: Sunnyvale, CA, 1998.

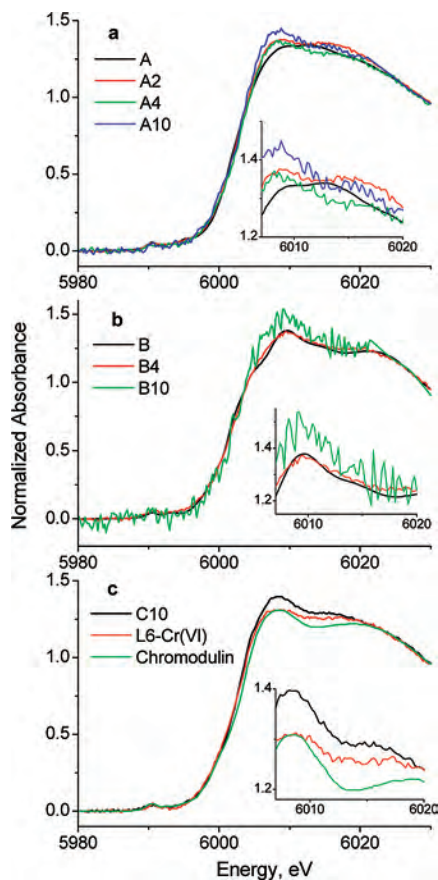


Figure 1. Typical changes in XANES spectra (295 K) of the Cr(III) complexes **A** and **B** after reactions with biological media (a and b) and a comparison of XANES spectra of Cr(III)- and Cr(VI)-treated rat muscle cells (L6) with published data for chromodulin (c).¹² Designations of the complexes (letters) and reaction conditions (numbers) correspond to those in Tables 1–3. A detailed comparison of XANES spectra is given in Figures S2–S4, Supporting Information. Insets are enlargements of the main XANES peaks.

or in aqueous buffers), using a Varian SpecAA-800 spectrometer. In the both cases, the samples were digested using ultrapure HNO₃ (69% w/v in H₂O, Merck), and spectrometer calibrations were performed with standard Cr(III) solutions (Aldrich). Protein concentrations in the cell pellets were determined by the Coomassie dye method, using bovine serum albumin as a standard.⁴² The pH values were measured by an Activon 210 ionometer with an AEP 321 glass/calomel electrode.

Results

XANES Spectroscopy of Cr(III) Nutritional Supplements in Biological Media. Typical changes in XANES spectra of the Cr(III) complexes **A–C** (Table 1) after the reactions with a range of natural and simulated biological fluids, as well as with cultured rat muscle cells (see the list of experimental conditions in Table 2), are shown in Figure 1, and a detailed comparison of XANES spectra is given in Figures S2–S4 (Supporting Information). No significant changes occurred in the spectrum of **A** after the reaction with simulated gastric juice (pH ~ 2)²⁵ for 24 h at 310 K (**A1** in Table 2 and Figure S2a, Supporting Information), while the

reaction of **A** with simulated intestinal fluid (pH ~ 8; 24 h at 310 K)²⁵ led to obvious spectral changes (**A2** in Table 2 and Figure 1a and S2a, Supporting Information). Mass spectrometry (ESMS) experiments under conditions close to those for **A2** showed the formation of di- and mononuclear Cr(III) complexes with EtCOO⁻/OH⁻ ligands (Figure S5 and Table S1 in the Supporting Information). Neither acidic (pH ~ 2) nor weakly basic (pH ~ 8) solutions caused significant changes in the XANES spectrum of **B** (**B1** and **B2** in Table 2 and Figure S2b, Supporting Information). On the other hand, reactions of **A** or **B** under artificial gastric and intestinal digestion conditions in the presence of a semisynthetic meal caused small but significant changes in the XANES spectra of both Cr(III) complexes (**A3**, **A4**, **B3**, and **B4** in Table 2, Figure 1a,b, and Figure S2c,d, Supporting Information). Notably, the presence of a semisynthetic meal altered the pattern of change in the XANES spectrum of **A** (compare the spectra **A** vs **A2** with **A** vs **A4** in Figure 1a).

Reactions of **A** with rat serum at 310 K caused significant time-dependent changes in XANES spectra (reaction times 1, 6, or 24 h; **A5–A7** in Table 2 and Figure S2e, Supporting Information). Similar spectral changes were observed in blood plasma, which was separated after the reaction of **A** with whole rat blood (24 h at 310 K, **A8** in Table 2 and Figure S2e, Supporting Information). The levels of Cr in the isolated RBC fraction after the reaction of **A** with blood were too low for detection by XANES spectroscopy. Significant changes occurred in the XANES spectrum of **B** after the reaction with rat serum for 1 h at 310 K, but further reaction for up to 24 h resulted in little change to the spectra (**B5–B7** in Table 2 and Figure S2f, Supporting Information).

Treatments of differentiated L6 rat muscle cells with freshly prepared solutions of Cr(III) compounds **A–C** in a complete cell culture medium (20 h at 310 K) led to significant changes in the XANES spectra of Cr(III) species detected both in the medium after the treatment and in the cell pellet (**A9–C9** and **A10–C10** in Table 2 and Figure 1 and Figure S3a–c, Supporting Information). Typical values of cellular Cr(III) uptake under these conditions, measured by GFAAS, were $0.5 \pm 0.1 \mu\text{g}$ of Cr/mg of protein for **A** and **C** and $0.2 \pm 0.1 \mu\text{g}$ of Cr/mg of protein for **B**. Preincubation of compounds **A–C** with the cell culture medium for 24 h at 310 K prior to the treatment of cells with the resultant cell culture medium led to a drastic reduction (by about 2 orders of magnitude) in the amounts of Cr in the cell pellet (as detected by XANES spectroscopy; a typical example for **C** is shown Figure S6, Supporting Information). The spectra of cell pellets after the treatments with the compounds **A–C** were similar, although not identical, to each other (Figure S3d, Supporting Information). By contrast, XANES spectra of Cr(III)-treated L6 cells were obviously different from those of Cr(VI)-treated L6 cells, as well as from published spectroscopic data for a purported natural Cr(III)-containing peptide, chromodulin (Figure 1c and Figure S3e, Supporting Information).³⁸ The XANES spectrum of Cr(VI)-treated L6 cells was essentially identical to those reported previously¹² for other Cr(VI)-treated mammalian cells (Figure S3e, Supporting Information),

(42) *Bio-Rad Protein Assay (technical bulletin)*, Cat. No. 500-0002; Bio-Rad Laboratories: Hercules, CA.

Table 3. Results of Multiple Linear Regression Fitting of XANES Spectra of Cr(III) in Biological Samples^a

sample	model						Cr-RSA ^b	R ²
	A	B	D	E	F	G		
A1	1.00(2)							0.99959
A2	0.84(1)				0.16(1)			0.99961
A3	1.00(1)							0.99939
A4	0.20(3)		0.23(2)		0.11(1)		0.46(3)	0.99957
A5	0.51(2)		0.13(1)		0.060(7)		0.30(2)	0.99983
A6	0.31(2)		0.17(1)		0.083(7)		0.44(2)	0.99983
A7	0.16(2)		0.22(1)		0.095(7)		0.52(2)	0.99982
A8			0.20(1)		0.11(1)		0.69(1)	0.99976
A9			0.35(2)		0.09(1)		0.56(2)	0.99914
A10			0.31(2)		0.13(2)		0.56(2)	0.99907
B1		1.00(1)						0.99945
B2		1.00(1)						0.99989
B3		0.76(3)					0.24(3)	0.99866
B4		0.56(2)	0.22(2)				0.22(1)	0.99968
B5		0.50(2)					0.50(2)	0.99929
B6		0.29(3)	0.23(2)				0.48(2)	0.99928
B7		0.16(3)	0.40(3)				0.44(2)	0.99898
B9		0.39(1)	0.49(1)			0.12(1)		0.99979
C10			0.43(6)				0.57(6)	0.99256
C9			0.44(2)			0.56(2)		0.99925
C10			0.31(3)	0.26(3)	0.12(1)		0.31(2)	0.99962
L6-Cr(VI) ^c			0.51(3)	0.36(2)	0.13(1)			0.99969

^a Shown in the table are calculated molar components of each of the contributing model complexes (Table 1) and the correlation coefficient (R^2). None of the optimized models included compound **C** (Table 1). Designations of the samples correspond to Tables 1 and 2 (the letters designate the Cr compounds, and the numbers designate the treatment conditions). Errors in the last significant figures are given in parentheses. Overlays of experimental and calculated spectra for each of the samples are shown in Figure 2 and Figure S8 (Supporting Information). ^b Rat serum albumin (5.0 mg mL⁻¹) was reacted with the corresponding Cr(III) compound (**A–C**, 1.0 mM) in HBS for 24 h at 310 K; then, the unbound Cr(III) was removed by membrane filtration (see the Experimental Section). The resulting samples are designated **A11**, **B11**, and **C11** in Figure S4 (Supporting Information). Due to the high noise level in the XANES spectrum of **B11**, smoothed spectral data were used in the fits (Figure S4a, Supporting Information). ^c Differentiated rat muscle cells (L6) were treated with [CrO₄]²⁻ (10 μM) in a complete medium for 20 h at 310 K, and cell pellets were prepared for XANES spectroscopy as described previously.¹²

despite the differences in treatment conditions (10 μM Cr(VI) for 20 h for L6 cells vs 100 μM for 4 h for other cell lines) and data collection at different beamlines (SSRL or ANBF).

Many of the observed XANES spectra of Cr(III) species in biological media differed from those of the original Cr(III) complexes by increased absorbances in the 6005–6020 eV region (e.g., **A10**, **B10**, and **C10** in Figure 1 or **B5–B7** in Figure S2f, Supporting Information). This increase was not matched by any of the model Cr(III) complexes used in the previous studies.¹² However, similar increases in Cr K-edge XANES absorbance were observed for the reactions of Cr(III) complexes with various biological macromolecules in vitro (Levina, unpublished data). In this work, complexes **A–C** were reacted with the two most abundant blood serum proteins (albumin and apo-transferrin)⁴³ in a buffered saline solution (HBS, pH 7.4, 24 h at 310 K), then unbound Cr(III) was removed by membrane filtration (condition set 11 in Table 2). The XANES spectra of Cr(III) adducts with rat serum albumin (**A11–C11**), shown in Figure S4 (Supporting Information), were used in multiple linear regression analyses along with those of model Cr(III) compounds (see below). Due to the high noise level in the spectrum of **B11**, a smoothed spectrum was used for the analyses (Figure S4a, Supporting Information). The spectra of Cr(III) adducts with bovine apo-transferrin were similar to those of the corresponding albumin adducts (Figure S4b–d, Supporting Information).

Modeling of Cr K-Edge XANES Spectra of Cr(III) in Biological Samples. The previously developed library of XANES spectra of model Cr(III) compounds with a wide range of biologically relevant donor groups (total of 17 compounds)¹² was used for multiple linear regression analyses of spectral data for **A–C** (Table 1) under the conditions listed in Table 2. As in the previous work,¹² most of the models were rejected in the preliminary analyses due to negative regression coefficients, and Cr(III) complexes with amino acid (L-aspartato and L-histidinato) and hydroxo ligands (**D–F** in Table 1) were included in the final fits (Table 3), along with the initial Cr(III) complexes (**A** and **B** in Tables 1 and 3; none of the fits contained model **C**). A comparison of XANES spectra of model Cr(III) compounds (**A–G** in Table 1) is shown in Figure S4e,f (Supporting Information). However, no satisfactory fits for most of the spectra of Cr(III) in biological samples could be obtained using these well-characterized models alone. Similarly, in the previous work,¹² no satisfactory fits were obtained for some of the spectra of Cr(III) in subcellular fractions (in contrast to the Cr(III) species in intact Cr(VI)-treated cells), since these samples were affected by hydrolysis. Therefore, the model library¹² was expanded by the inclusion of (i) Cr(III) complexes with rat serum albumin (**A11–C11** in Figure S4, Supporting Information; Cr-RSA in Table 3), which model Cr(III) interactions with biological macromolecules, and (ii) Cr(III) aqua/hydroxo oligomers (**G** in Table 1), which are likely to form by the hydrolysis of Cr(III) complexes in neutral aqueous solutions.²³ Complexes **A11–C11** could be replaced in the models (Table 3) by the

(43) Sanz-Medel, A.; Soldado Cabezuolo, A. B.; Milačič, R.; Bantan Polak, T. *Coord. Chem. Rev.* **2002**, *228*, 373–383.

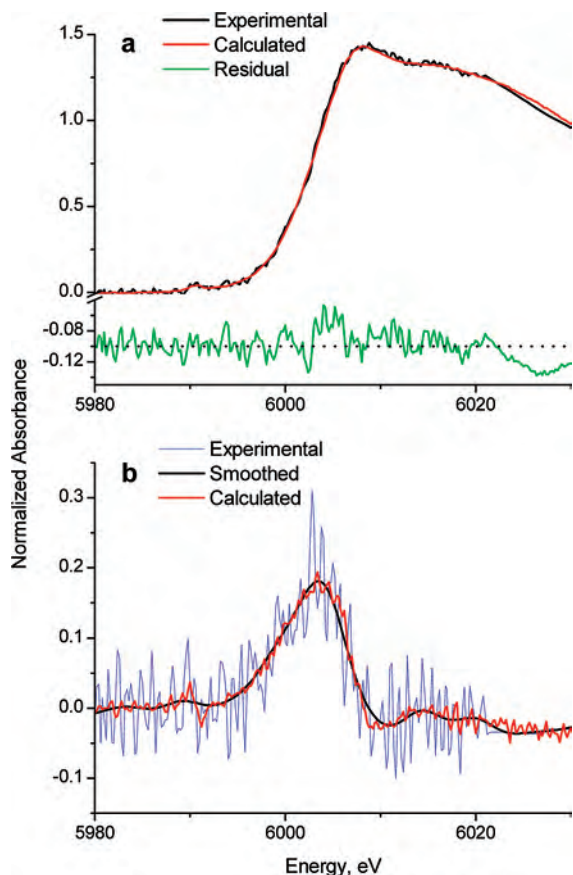


Figure 2. Typical results of multiple linear regression analyses of the K-edge XANES spectra of Cr(III) in biological systems (sample **A10** in Tables 1 and 2; original spectrum, a; and first-derivative spectrum, b). The applied model corresponds to that in Table 3. The scale for the residual spectrum in part a is expanded 5-fold compared with the experimental and calculated spectra. Smoothing of the first-derivative XANES spectrum (b) was performed by the FFT procedure³⁵ with a 20-point window^{11c} (see the Experimental Section). Overlays of experimental and fitted spectra for all of the samples listed in Table 3 (including the first-derivative spectra) are shown in Figure S8, Supporting Information.

corresponding Cr(III)-transferrin adducts (Figure S4b–d, Supporting Information), with no significant changes in the final fits. Species **G** were generated by the reactions of $[\text{Cr}(\text{OH})_2]^{3+}$ with one molar equivalent of NaOH, followed by gel-filtration chromatography (see the Experimental Section). The main chromatographic fraction contained predominantly dimeric and trimeric species,²³ which were stable under the sample preparation conditions, including freeze-drying (as shown by electronic absorption spectroscopy; Figure S7 and Table S2 in the Supporting Information). The other two chromatographic fractions, containing predominantly monomeric and polymeric Cr(III) species (Figure S7 and Table S2, Supporting Information),²³ were unstable during freeze-drying and were not used in further studies.

The use of models **A–G** (Table 1 and Figure S4e,f, Supporting Information) along with Cr(III)–RSA adducts (**A11–C11** in Figure S4a–d, Supporting Information) in multiple linear-regression analyses led to good fits for all of the XANES spectra of Cr(III) in biological samples (conditions 1–10 in Table 2), with the differences between experimental and fitted spectra in most cases not exceeding double the noise levels. A typical spectral fit (both the

original and first-derivative spectra for sample **A10**) is shown in Figure 2, and fits for all of the other samples are shown in Figure S8, Supporting Information. Unlike for the biotransformation products of potential antidiabetic Mo(VI) complexes,^{11c} the first derivatives of XANES spectra for Cr(III) species in biological samples were relatively uninformative, dominated by the maxima corresponding to the edge jump, while smaller maxima at higher energies were often indistinguishable from the noise (Figure 2b and Figure S8, Supporting Information).

Taken together, the XANES fitting results for the reaction products of **A–C** with biological media (Table 3) point to ligand-exchange reactions with amino acids (models **D** and **E**) and biological macromolecules (modeled by rat serum albumin, Cr-RSA in Table 3), as well as to hydrolysis leading to aqua/hydroxo complexes (models **F** and **G** in Table 3). As expected, the extent of ligand-exchange reactions was higher after the combined artificial gastric and intestinal digestion (samples **A4** and **B4** in Table 3) compared with the gastric digestion alone (samples **A3** and **B3** in Table 3), and only the combined digestion led to the appearance of Cr(III) amino acid complexes. Small spectral changes that occurred under condition **A3** (Figure S2c) could not be matched by any combination of the spectra of the model complexes (Table 3). Extensive formation of Cr(III) amino acid complexes was suggested by fitting the spectra of the reaction products of **A–C** with a cell culture medium (20 h at 310 K; samples **A9–C9** in Table 3). Time-dependent measurements for the reactions of **A** or **B** with undiluted rat serum (samples **A5–A7** and **B5–B7** in Table 3 and Figure S2e,f, Supporting Information) showed a gradual replacement of the initial Cr(III) complex with ligand-exchange products (Figure 3). As shown in Figure 3 and Figure S2e,f, Supporting Information, and in Table 3, changes in the coordination environment of **A** during the reaction with serum were more gradual than those for **B**, where most of the changes (predominantly Cr(III) binding to serum proteins) occurred during the first hour of reaction. These changes were probably accelerated by the sonication that was required to dissolve **B** in the serum (see the Experimental Section). For all of the samples of Cr(III)-treated L6 cells (**A10**, **B10**, and **C10** in Table 3 and Figure 1), the fits to the XANES data suggested the absence of the initial Cr(III) compound (**A**, **B**, or **C**, respectively) and the presence of significant amounts of Cr(III) amino acid and protein complexes. Finally, the fitting results for Cr(VI)-treated L6 cells (L6–Cr(VI) in Table 3 and Figure 1c), including the Cr(III) aspartato (**D**), histidinato (**E**), and hydroxo (**F**) complexes in a ~4:3:1 molar ratio, were in close agreement with the data for other Cr(VI)-treated mammalian cells.¹²

XAFS Spectra of Cr(III) in Biological Samples. A comparison of Fourier-transform XAFS spectra of **A** (trinuclear Cr(III) propionate, Table 1) in the solid state and in aqueous solutions (Figure 4) points to a decrease in intensity of Cr–Cr interactions (indicated with asterisks) following the reactions with artificial intestinal fluid (**A2**) or with rat serum (**A7**). On the other hand, these interactions did not disappear completely, as shown by comparison with a typical

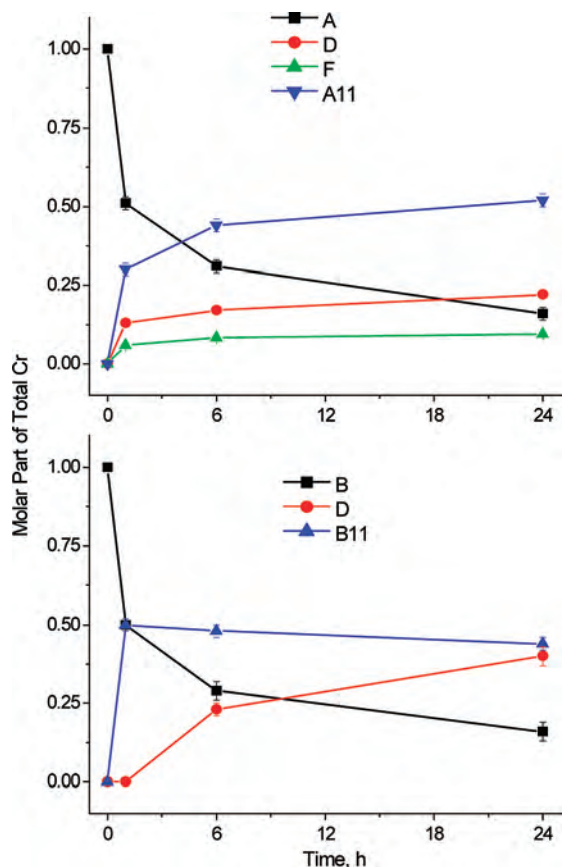


Figure 3. Time-dependent changes in the composition of Cr(III) species during the reactions of **A** or **B** with rat serum, as determined by multiple linear-regression analyses of XANES spectra (samples **A5**–**A7** and **B5**–**B7** in Table 3 and Figure S2e,f, Supporting Information). Designations of the model complexes (**A**, **B**, **D**, and **F**) correspond to those in Table 1; **A11** and **B11** are adducts of **A** and **B** with rat serum albumin (see the Experimental Section and Figure S4a–d, Supporting Information).

mononuclear Cr(III) complex, **D** (Figure 4 and Table 1). These observations are supported by a decrease in average number of Cr–Cr interactions per molecule in the samples **A2** and **A7** compared with **A** (solid) and **A1** (the n values shown in Figure 4), as determined by SS XAFS fittings (red lines in Figure 4). Detailed fitting results, as well as experimental and fitted XAFS spectra (non-Fourier-transformed), are shown in the Supporting Information (Table S3 and Figure S9, respectively). For all of the spectra, the best fits of the first coordination shells included six O/N donor atoms at an average distance of 1.96 ± 0.02 Å from the central Cr atom (Table S3, Supporting Information). Relatively poor fits were obtained by SS XAFS calculations (Table S3, Supporting Information; $R = 25$ – 32% ; fits with $R < 20\%$ are usually considered satisfactory)^{11a,31} due to significant multiple-scattering (MS) contributions of carboxylato groups to the spectra of **A** and its derivatives.¹² The introduction of extra SS shells (e.g., C atoms)³⁸ into the models did not lead to statistically significant improvements of the fits.^{11a} No attempts were made to perform MS XAFS fits to the data from the reaction products of **A** in biological media, since these samples are likely to contain complex mixtures of Cr(III) species (Table 3).

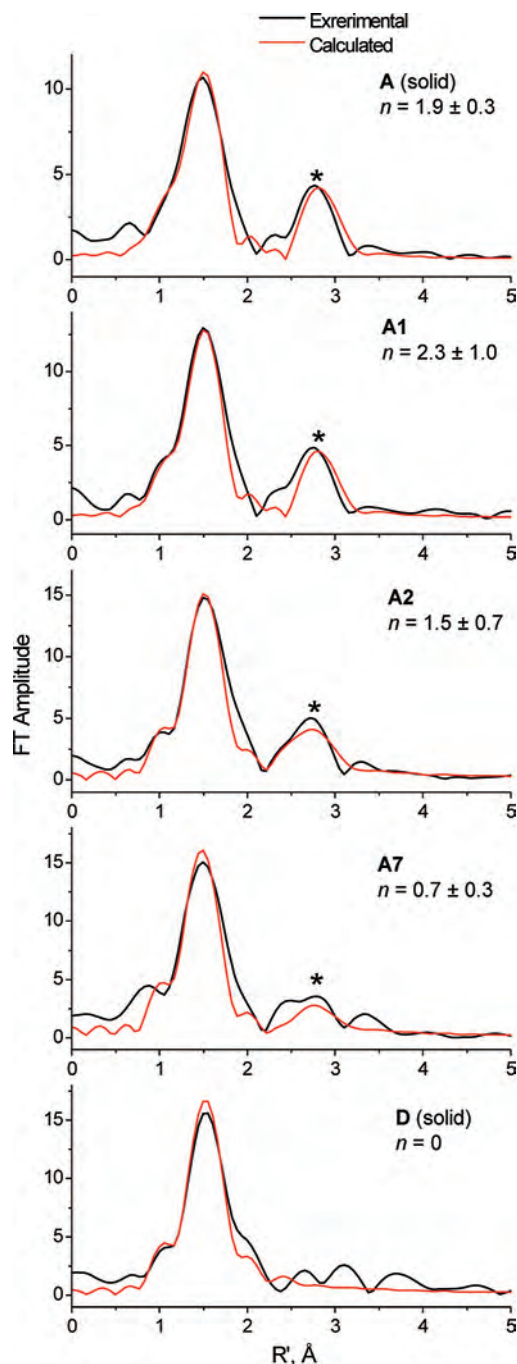


Figure 4. Fourier transforms of XAFS spectra (295 K) of **A** and **D** (solid mixtures with BN) and reaction products of **A** in biological media (**A1**, **A2**, and **A7**, freeze-dried solids). Designations of the samples correspond to those given in Tables 1–3. Peaks due to Cr–Cr interactions are designated with asterisks. The n values are the average numbers of Cr–Cr interactions per Cr, calculated by SS XAFS analyses (details are given in Figure S9 and Table S3, Supporting Information). Standard deviations in the n values, arising from the noise of the data, were calculated by Monte Carlo analysis.³²

Oxidation Reactions of Cr(III) Complexes in Biological Media. The ability of **A** (and to a lesser extent those of **B** and **C**) to react with biological oxidants such as H_2O_2 or oxidase enzymes in neutral aqueous solutions with the formation of a known carcinogen, Cr(VI), has been demonstrated previously.¹⁵ It was also noticed that **A** could be oxidized to Cr(VI) by H_2O_2 in undiluted bovine serum.¹⁵ In this work, the reactivities of **A** and **B** toward biological

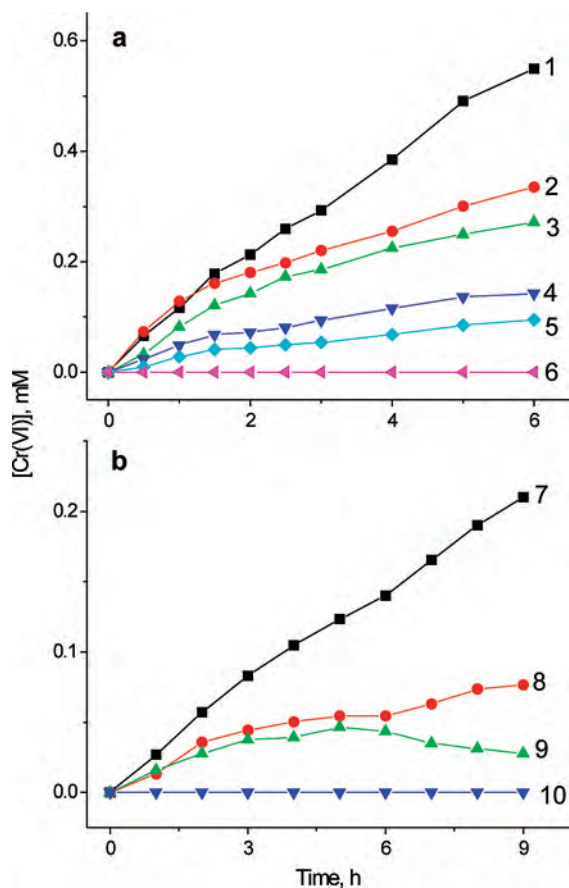


Figure 5. Typical kinetic curves of Cr(VI) formation (measured spectrophotometrically with diphenylcarbazide, see the Experimental Section) for the reactions of **A** or **B** (1.0 mM Cr) with H₂O₂ (5.0 mM, a) or with glucose oxidase (5.0 U mL⁻¹, b) in undiluted rat serum or in aqueous buffer (HBS, pH = 7.4) at 310 K. Designations of the curves: (1) **A** in HBS, (2) **A** in serum, (3) **B** in serum, (4) **B** in serum, preincubated for 24 h at 310 K prior to the addition of H₂O₂, (5) **A** in serum, preincubated for 24 h at 310 K prior to the addition of H₂O₂, (6) **B** in HBS, (7) **A** in HBS in the presence of glucose (5.0 mM), (8) **B** in serum, (9) **A** in serum, and (10) **B** in HBS in the presence of glucose (5.0 mM).

oxidants in an aqueous buffer (HBS, pH = 7.4) and in undiluted rat serum were compared; typical results are presented in Figure 5. Most remarkably, complex **B** was oxidized to Cr(VI) at a significant rate by both H₂O₂ and the glucose oxidase/glucose/O₂ system in serum (curves 3 and 8 in Figure 5), while the corresponding reaction rates in HBS were negligibly low (curves 6 and 10 in Figure 5). This difference in reactivity was confirmed by the detection of a characteristic Cr(VI) signal ($\lambda_{\max} = 372 \text{ nm}$)¹⁵ in the electronic absorption spectra of the reaction products of **B** and H₂O₂ in serum, while no such signal was observed for the reaction mixtures in HBS (Figure S10 in Supporting Information).

The reaction rate for the oxidation of **B** (1.0 mM) with H₂O₂ (5.0 mM) in rat serum increased during the first hour of reaction (curve 3 in Figure 5), while the oxidation rate of **A** steadily decreased under the same conditions (curve 2 in Figure 5). Preincubation of **A** or **B** with serum for 24 h at 310 K prior to the addition of H₂O₂ decreased the reaction rates compared with the reactions of freshly added Cr(III) complexes (curves 4 and 5 vs 2 and 3 in Figure 5). For both oxidation systems used, the highest reaction

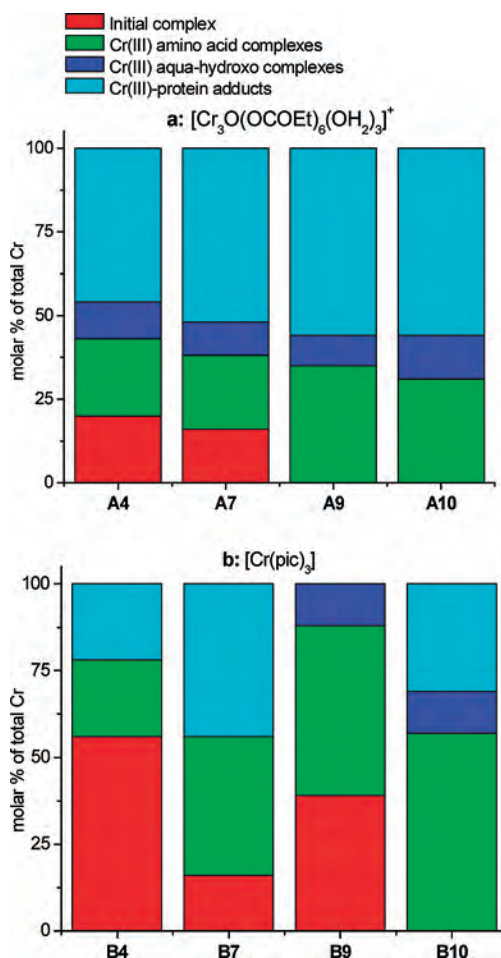


Figure 6. Typical changes in coordination environments in the products of reactions of Cr(III) nutritional supplements ($[\text{Cr}_3\text{O}(\text{OCOEt})_6(\text{OH}_2)_3]^+$ (a) or $[\text{Cr}(\text{pic})_3]$ (b) with biological media, determined by multiple linear regression analyses of XANES spectra with the use of a library of model Cr(III) compounds (based on the data of Table 3). Designations of the samples correspond to those in Tables 1–3.

rates were observed for complex **A** in HBS (curves 1 and 7 in Figure 5).

Discussion

Reactivities of the Cr(III) complexes **A–C** under various biologically relevant conditions can be conveniently studied by XANES spectroscopy (Figure 1 and Figures S2–S4, Supporting Information), and the chemical nature of the observed spectral changes can be inferred from multiple linear-regression analyses, using a library of model Cr(III) compounds¹² (Figure 2 and Figure S8, Supporting Information, and Table 3). A detailed description of these changes is given in the Results section, and similarities and differences in the reactivities of the studied Cr(III) complexes are summarized in Figure 6 and in the text below.

A known biologically active complex, trinuclear Cr(III) propionate (**A**),^{2,6} was stable under simulated gastric conditions (pH ~ 2), in agreement with suggestions in the literature (**A1** and **A3** in Table 3).⁷ On the other hand, complex **A** underwent significant changes under simulated intestinal conditions (pH ~ 7–8; **A2** and **A4** in Table 3). These involved base hydrolysis (with the formation of hydroxo

complexes; model **F** in Table 3), as well as a binding of **A** to the components of a semisynthetic meal, such as amino acids and proteins (models **D** and Cr-RSA in Table 3). Similar ligand-exchange reactions occurred between **A** and blood serum or a cell culture medium (**A5–A9** in Table 3). The coordination environment of Cr(III) in an insulin-sensitive muscle cell line (L6), treated with **A**, was very different from that in the original compound (**A10** in Table 3 and Figure 1a). Thus, contrary to suggestions in the literature,⁴⁴ compound **A** did not enter cells intact, and cellular uptake of this compound was not significantly higher than that of an inorganic Cr(III) salt such as **C** (as shown by GFAAS measurements, see the Results). As expected,^{10,45} a highly acidic Cr(III) salt **C** was converted in a cell culture medium into a mixture of aqua/hydroxo and amino acid complexes (**C9** in Table 3).

A widely used nutritional supplement, Cr(III) picolinate (**B**),^{1–5} which is usually regarded as relatively stable under biological conditions,^{15,46} underwent ligand-exchange reactions with artificial digestion systems (although only in the presence of a semisynthetic meal; **B1–B4** in Table 3), as well as with blood serum and with a cell culture medium (**B5–B9** in Table 3). The coordination environment of Cr(III) in L6 cells, treated with **B**, was also different from that in the original compound (**B10** in Table 3 and Figure 1b), but a detailed analysis of these data was difficult due to a high noise level in the spectrum. Previously, the ability of cultured liver cells and experimental animals to metabolize **B** was demonstrated by chromatographic and radiolabeling techniques.⁴⁷ Generally, **B** appeared to undergo ligand-exchange reactions predominantly in amino acid rich media and was less susceptible to base hydrolysis compared with **A** (which is readily explained by the presence of aqua ligands in the latter complex).⁴⁵

Most remarkably, reactions of **B** with blood serum led to a dramatic increase in reactivity of the resultant Cr(III) species toward biological oxidants (H₂O₂ or glucose oxidase system; Figure 5). This finding supports the hypothesis^{10,12} that biological oxidation of Cr(III) complexes, including **B**, to Cr(VI) is a major source of both their antidiabetic activity and their potential genotoxicity. By contrast, the reactivity of **A** toward oxidants was decreased, although not completely abolished, by the interactions with serum (Figure 5). Similar reactivities of **A** and **B** toward oxidants in serum, in contrast with their vastly different reactivities in a buffer solution (Figure 5), are in agreement with the data of Table 3 and Figure 6, which suggest that similar Cr(III) species (predominantly amino acid and protein complexes) are formed in blood serum starting from either **A** or **B**. Importantly, the

increased ease at which the biotransformation products of [Cr(pic)₃] are oxidized to genotoxic Cr(VI) in comparison to the supplement itself (Figure 5) raises serious concerns as to the safety of [Cr(pic)₃] when taken in large amounts (i.e., the doses required to observe antidiabetic effects are far in excess of the recommended daily intake⁴ and are more likely to produce significant amounts of genotoxic Cr(VI) in vivo, which can overcome the cellular detoxification mechanisms²⁹).

In this and previous¹² studies, XANES spectra of Cr(III) species formed in Cr(VI)-treated mammalian cells were successfully fitted with a combination of well-defined models, including Cr(III) amino acid and hydroxo complexes (e.g., the last row in Table 3). By contrast, fits to the XANES spectra of Cr(III)-treated cells (**A10**, **B10**, and **C10** in Table 3 and Figure 1) had to include the adducts of the corresponding Cr(III) complexes with rat serum albumin (Cr-RSA in Table 3) as additional models. The likely nature of these adducts (characterized by increased absorbances at 6005–6020 eV in XANES spectra; **A11–C11** in Figure S4, Supporting Information) as polynuclear Cr(III) complexes adsorbed onto biological macromolecules is supported by the following observations: (i) the shapes of the XANES spectra were more dependent on the nature of the initial Cr(III) complex (**A**, **B**, or **C**) than on the nature of the protein (RSA or bovine apo-transferrin; Figure S4a–d, Supporting Information), and (ii) the spectrum of a mixture of hydrolytic dimers/trimers (**G** in Table 1) was closer to those of the Cr-RSA adducts than any of the spectra of the model Cr(III) compounds used in the previous work¹² (Figure S4a, Supporting Information). Therefore, the presence of significant proportions of the Cr-RSA models in the fits of XANES spectra of Cr(III)-treated L6 cells (**A10–C10** in Table 3 and Figure 6) suggests that at least part of Cr(III) found in the cell pellets was bound to macromolecules at the cell surface, rather than taken into the cytoplasm. When **A** or **C** were allowed to bind to the components of the cell culture medium for 24 h at 310 K prior to the treatment of cells, no significant cellular uptake of Cr was observed (Figure S6 in Supporting Information). Thus, the addition of easily hydrolyzable Cr(III) complexes, such as **A** or **C**, to cultured cells causes Cr(III) binding to the macromolecules of cell membranes, which is probably responsible for the reported “efficient uptake” of **C** by mammalian cells,⁴⁸ as well as for at least some of the reported effects of this and other Cr(III) compounds on cell signaling.⁹

The close similarity of XANES spectra obtained for Cr(III) adducts with either albumin or transferrin (Figure S4b–d, Supporting Information) does not enable us to assign Cr(III) binding in serum to a certain type of protein (samples **A5–A7** and **B5–B7** in Table 3). This uncertainty may be due to the fact that the concentration of Cr (1.0 mM) used in these experiments was at least an order of magnitude higher than that required for specific Cr(III) interactions with the metal binding sites of transferrin.⁴³

(44) (a) Shute, A. A.; Chakov, N. E.; Vincent, J. B. *Polyhedron* **2001**, *44*, 2241–2252. (b) Shute, A.; Vincent, J. B. *J. Inorg. Biochem.* **2002**, *89*, 272–278. (c) Clodfelder, B. J.; Chang, C.; Vincent, J. B. *Biol. Trace Elem. Res.* **2004**, *98*, 159–168.

(45) Levina, A.; Lay, P. A. *Coord. Chem. Rev.* **2004**, *249*, 281–298.

(46) (a) Gammelgaard, B.; Jensen, K.; Steffansen, B. *J. Trace Elem. Med. Biol.* **1999**, *13*, 82–88. (b) Sun, Y.; Ramirez, J.; Woski, S. A.; Vincent, J. B. *J. Biol. Inorg. Chem.* **2000**, *5*, 129–136.

(47) (a) Kareus, S. A.; Kelley, C.; Walton, H. S.; Sinclair, P. R. *J. Hazard. Mater.* **2001**, *B84*, 163–174. (b) Hepburn, D. D.; Vincent, J. B. *Chem. Res. Toxicol.* **2002**, *15*, 93–100.

(48) Blankert, S. A.; Coryell, V. H.; Picard, B. T.; Wolf, K. K.; Lomas, R. E.; Stearns, D. M. *Chem. Res. Toxicol.* **2003**, *16*, 847–854.

In summary, XANES spectroscopic studies (Figure 6), in combination with XAFS, ESMS, and kinetic data, showed that the currently used Cr(III) nutritional supplements, including the purportedly inert $[\text{Cr}(\text{pic})_3]$ complex,⁴⁶ undergo extensive ligand-exchange reactions in biological media, which are likely to affect their gastrointestinal absorption and subsequent metabolism. These processes include the formation of genotoxic Cr(VI) species in the reactions with biological oxidants, which enhances the current concern over the safety of using $[\text{Cr}(\text{pic})_3]$ and other Cr(III) complexes as nutritional supplements.^{4,10} Reactivity of Cr(III) compounds in cell culture media has to be taken into account when the effects of these compounds on cultured cells are considered. As is the case for Cr(VI)-treated mammalian cells,¹² the use of a library of XANES spectra of model Cr(III) compounds was proven to be a powerful tool in studies of the changes in the coordination environments of Cr(III) nutritional supplements in biological media. The developed library can also be used for other purposes, such as the studies of Cr(III) compounds formed in plant or microbial biomass during the bioremediation of Cr(VI).⁴⁹

Acknowledgment. The research was supported by Australian Research Council (ARC) Discovery Grants (DP0208409 and DP0774173), an ARC Professorial Fellowship (DP0208409) to P.A.L., and an ARC LIEF grant (LE0346515) for the 36-pixel Ge detector at ANBF. I.M. is grateful to the Chemistry Department, Bandung Institute of Technology, Indonesia, for partial funding of her postgraduate studies at The University of Sydney and for funding from the ARC Discovery grant. X-ray absorption spectroscopy was performed partially at

ANBF with support from the Australian Synchrotron Research Program (ASRP), which is funded by the Commonwealth of Australia under the Major National Research Facilities program, and partially at SSRL, which is operated by the Department of Energy, Office of Basic Energy Sciences. The SSRL Biotechnology Program is supported by the National Institutes of Health, National Center for Research Resources, Biomedical Technology Program, and by the Department of Energy, Office of Biological and Environmental Research. The research at SSRL was also supported by the ASRP. We thank Dr. Amira Klip (The Hospital for Sick Children, Toronto, Canada) for providing a sample of L6 cells, Dr. Antonio Bonin (The University of Sydney) for providing samples of rat blood, Dr. Hugh Harris (The University of Sydney) for the assistance with XAS experiments and helpful advice on the XANES data analysis, and Drs. Garry Foran and Matthew Latimer for the assistance with XAS experiments at ANBF and SSRL, respectively.

Supporting Information Available: (i) Typical examples of background subtraction and normalization of XANES spectra, (ii) a detailed comparison of XANES spectra of the complexes **A–C** before and after the reactions with biological media, (iii) XANES spectra of model Cr(III) compounds **A–G** (Table 1), (iv) typical ESMS data and assignment of major ESMS signals for the hydrolysis of **A** in neutral aqueous solutions, (v) electronic absorption spectroscopic data for Cr(III)–OH–OH₂ complexes in aqueous solutions, (vi) experimental and calculated XANES spectra of Cr(III) compounds in biological media (not included into the main text), (vii) experimental and fitted XAFS spectra of **A** and its reaction products with biological media, and (viii) typical electronic absorption spectra of the reaction products of **B** with H₂O₂ in aqueous buffer and in blood serum. This material is available free of charge via the Internet at <http://pubs.acs.org>.

IC7024389

(49) (a) Parsons, J. G.; Dokken, K.; Peralta-Videa, J. R.; Romero-Gonzalez, J.; Gardea-Torresdey, J. L. *Appl. Spectrosc.* **2007**, *61*, 338–345. (b) Bluskov, S.; Arocena, J. M.; Omotoso, O. O.; Young, J. P. *Int. J. Phytoremed.* **2005**, *7*, 153–165.